



Integrated seawater intrusion study of coastal region of Thiruvallur district, Tamil Nadu, South India

S. Senthilkumar¹ · K. Vinodh² · G. Johnson Babu² · B. Gowtham² · V. Arulprakasam³

Received: 7 September 2017 / Accepted: 13 June 2019 / Published online: 21 June 2019
© The Author(s) 2019

Abstract

The groundwater is the main resource of water for irrigation activity in river lacking area. The freshwater–seawater interface in the study region that has existed 3 km away from the coast in the year 1969 has been found to be migrated to distance of 13 km from the coast during the year 2007 noticed by the Central Ground Water Board (Central ground water board's district groundwater brochure, Thiruvallur district, Tamil Nadu, 2007). Integrated geochemical and geophysical techniques were carried out in the study area to decode subsurface geologic pattern and delineate the seawater–freshwater zones. Total numbers of 50 samples were collected from the entire study area and analyzed for major ions. The considerable samples are brackish scenery of groundwater water at low depth. Chadha and Piper's plots categorize the coastal groundwater into Na–HCO₃, Ca–Na–HCO₃, Ca–HCO₃, and Na–Cl water facies, with Ca–HCO₃ as the dominant. Cl/CO₃ + HCO₃ ratio, Cl/HCO₃, and ionic strength, Mg/Ca and Cl/HCO₃ ratios show that most of the samples in the study area are affected by seawater intrusion, which is also confirmed by the geophysical method. The results of vertical electrical sounding carried out in the study area reveal the low transverse resistance and high longitudinal conductance. It suggests the brackish nature of the groundwater in the eastern part of the study area may be due to the seawater intrusion. The final map using GIS platforms productively delineates the location that is really undergoing seawater and freshwater zone is migrated toward the inland. The article suggested further studies to arrest the migration of sea/freshwater interface into the land and avoid overexploitation of groundwater to further development.

Keywords Groundwater · Geochemical · Geophysical · Chadha · Overexploitation

Introduction

Coastal regions are generally vulnerable to seawater intrusion especially in regions where groundwater is over-pumped. Saline water interference is the main issue in coastal areas due to over-extraction of groundwater, and it directs to the devastation of the excellence of the freshwater aquifers. The level of seawater intrusion is influenced by the natural history of geological settings, hydraulic gradient, rate of groundwater extraction and its renew (Choudhury et al.

2001). It is important to recognize the extent of saline water intrusion in order to avoid the deterioration in groundwater quality. Heavy demand of water for various domestic, irrigation, industrial purposes and rainfall recharge less than the groundwater abstraction are the main causes of the decrease in groundwater level in the coastal aquifer (Nair et al. 2013). Saline water intrusion in the coastal region not only is affecting the communal and financial systems but also damages the whole environment of the affected region (Amores et al. 2013). The identification of seawater intrusion has been done by various methods including isotope studies, geochemical and geophysical studies (FAO 1997; Gnanasundar and Elango 1999; Kim et al. 2003; Gowtham 2003; Marimuthu et al. 2005; Richter and Krietler 1993; Davis et al. 1996; Sathish et al. 2011; Aris et al. 2007; Banerjee et al. 2012; CAMP 2000; Giménez-Forcada 2010, 2014; Najib et al. 2017;). The assessment of seawater intrusion in coastal aquifers from groundwater geochemistry has been successfully

✉ S. Senthilkumar
siva.senthil.geo@gmail.com

¹ Department of Earth Sciences, Pondicherry University, Puducherry, India

² Department of Geology, Presidency College (Autonomous), Chennai 600005, India

³ Central Ground Water Board, South East Coastal Region, Chennai, India

done by different authors (Pujari and Abhay 2009; Subba Rao 2002; Naik et al. 2007; Saxena et al. 2002, 2004, 2005).

The geophysical method is one of the useful techniques to differentiate the subsurface resistivity to identify the seawater intrusion. The huge differences among the resistivity of fresh water zone and saltwater zones have been used by numerous investigations for the resolve of seawater intrusion in various coastal regions (Choudhury et al. 2001; Koukadaki et al. 2007; Hodlur et al. 2010; Zohdy 1969; Sabet 1975; Respond 1990; and Frohlich et al. 1994).

The research boundary located an eastern coastal part of Thiruvallur district of Tamil Nadu in South India which is nearer to Chennai metropolitan city. Generally, the coastal area faces many problems in groundwater quality maintenance due to huge settlement along these zones, well-developed road network, densely agricultural activity, and groundwater overexploitation. The present study mainly deals with groundwater quality affected by seawater intrusion. The freshwater–seawater interface in the study area that has existed 3 km away from the coast in the year 1969 has been found to be migrated within a distance of 13 km

from the coast during the year 2007 (CGWB 2007). The present study is planned to recognize the extent of seawater into the coastal aquifer of entire Thiruvallur district by using hydrogeochemistry and geophysical techniques. Water quality study has been conceded for pre-monsoon 2012 and post-monsoons of 2013 from various wells in the study region. High electrical conductivity (EC) and sodium and chloride concentration in this area have motivated us to acquire geophysical investigation for delineating high-salinity zones from vertical electrical sounding (VES) method.

Study area

The study area that falls in the coastal region of Arani–Kortalaiyar river basin is situated between 13°00'N to 13°35'N latitude and 79°55' to 80°25'E longitude enclosed by Indian Toposheets No. 66 C 4, 66 C 3, 66 C 8 and 66 C 7 (Fig. 1). It is surrounded in the eastern region by the Bay of Bengal, the Western region covered by Poondi reservoir, Southern part covered by Kancheepuram and Chennai districts, and state

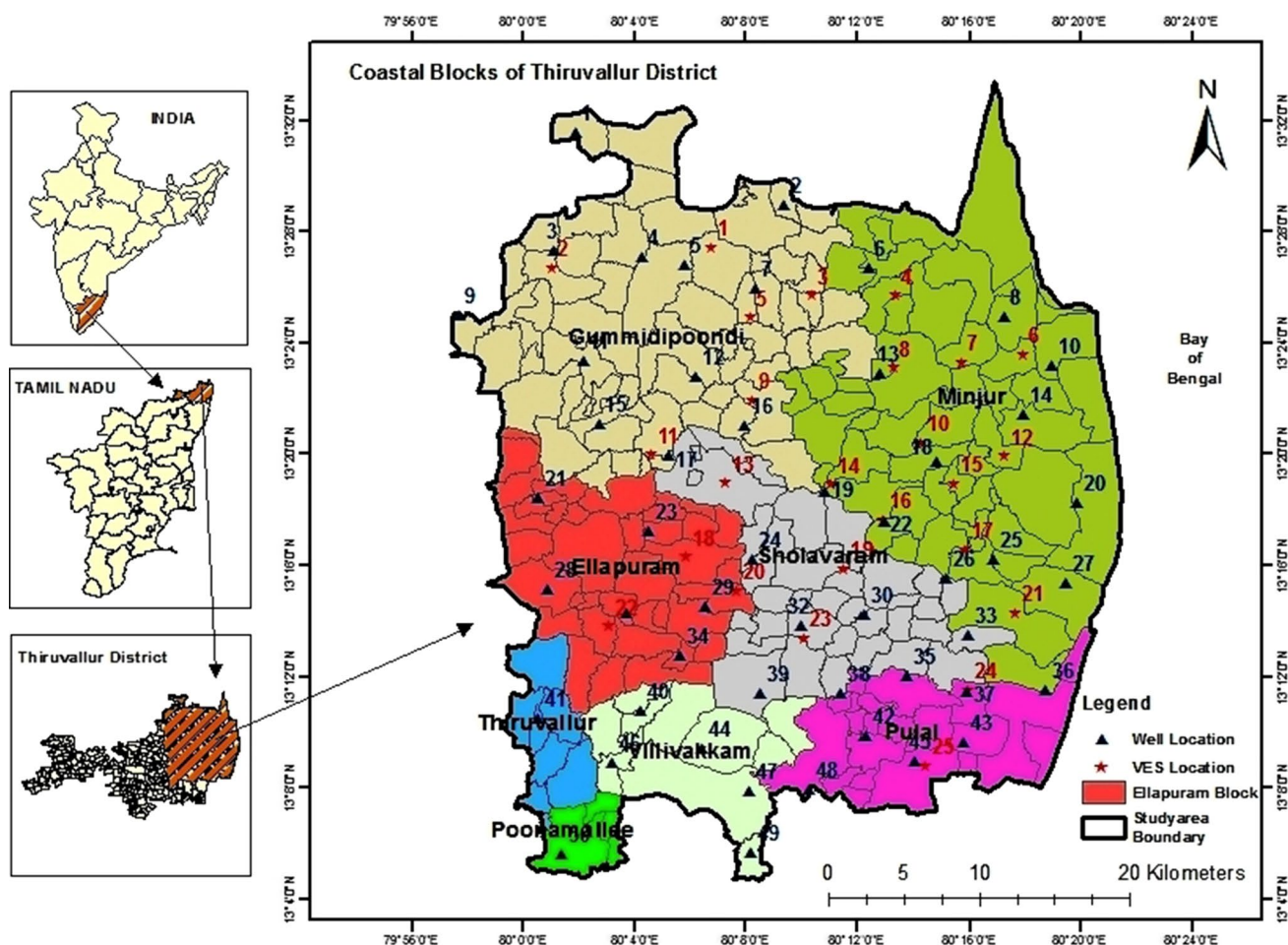


Fig. 1 Location map of the study area

of Andhra Pradesh is bounded in the northern part; the total area covered is 1402.79 sq km. Average annual rainfall in this area is 1200 mm which is caused by northeast monsoon (October–December). Generally, the study area receives rain due to both southwest monsoon and northeast monsoon. Sub-dendritic is the drainage pattern of the study area. The Arani River that flows in the northern part of this region and Koratalai River occupied by southern part are the major rivers flowing in the study area which is non-perennial in nature. In the eastern boundary, Buckingham Canal runs parallel to the sea and this carries saline water from the Bay of Bengal. The Pulicat Lake is situated in the northeastern side of the study region directly connected with the sea.

Geology and geomorphology

Geologically, the gneiss and Charnockite rocks of the Proterozoic era occur as basement arranging between 65 and 105 m (UNDP 1987). These rocks are overlain by the Gondwana formation of Jurassic to Lower Cretaceous rocks consisting of clay, shale, sandstone, conglomerate, and boulders

(Fig. 2a). The upper Gondwana sediments consist of two stages, viz. the lower Sriperumpudur stage consisting of fluviatile clays, shales, and feldspathic sandstones and the Satyavedu stage representing the marine sediments of ferruginous sandstones, conglomerates and boulders (GSI 2005). Tertiary formations overlay these with clays, shale, and sandstone. Alluvium of quaternary to recent period consisting of clay, silt, sand, gravel, and pebbles occurs at the top. The thicknesses of alluvium vary from 45 to 60 m, and it is high between the rivers and increases toward the coast. The alluvial deposits of about 60 m thickness are water-bearing and function as aquifers. Groundwater in the upper part of the alluvial formation with a huge amount of finer material with reasonably low hydraulic conductivity occurs in unconfined condition. The groundwater table is generally at a depth of about 5 to 7 m. The interlaying clay and silt of varying thickness (2–5 m) function as an aquitard, which is about 15 m in depth. The lower part of the alluvium with relatively high hydraulic conductivity functions as a semi-confined aquifer. The conglomerates with a sandy clayey matrix are hard and compact, and exposures of it are invariably strewn with gravel, pebbles, and boulders. The

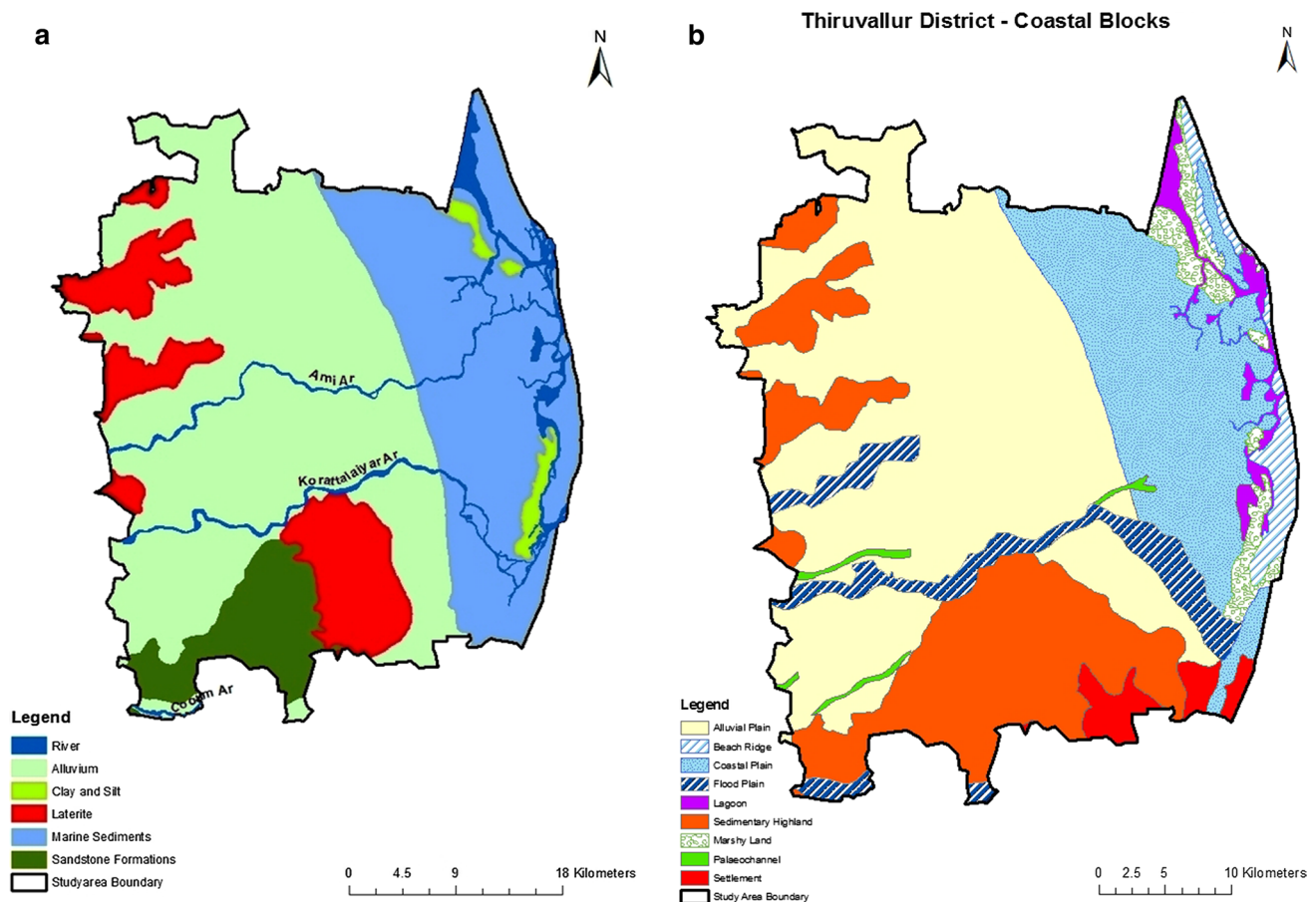


Fig. 2 a Geology map. b Geomorphology map

conglomerates and boulder beds occur nearer to the crystalline rocks with a total thickness exceeding 30 m.

The maximum altitude of the study area is in relation to 10 m in the west and sea level in the east. Thus, the area gently slopes toward east. There is no remarkable elevation difference in the north–south direction, except for the two river courses. Important geomorphic units include alluvial plains, shallow/deep pediments, pediplains, coastal plains/dunes and a number of paleochannels (Fig. 2b). Most of the area consists of alluvial plains, between the two rivers. Geomorphic evaluation and morpho-structural analysis of the area reported by the previous study suggest that the neo-tectonic activity during the Quaternary period resulted in marine regression, large-scale changes, and shifting in the courses of major rivers. The coastal landforms include estuarine, tidal, mud flats or lagoons and salt marsh. A few isolated beaches of 100 to 500 m widths occur along the coast.

Materials and methods

Groundwater sample collection and analysis

Groundwater sample collected in 50 locations from both open well and bore well is covering the entire study area in equal network projection. Groundwater samples were collected in fresh polyethylene bottles of 500 ml capability during pre-monsoon 2012 and post-monsoon 2013. The samples were analyzed for all major ions using the following standard methods (APHA 2005). Physicochemical parameters like pH, EC, and TDS were measured at the sample collection site using a water analysis kit (Deep Vision-191). Sodium (Na) and potassium (K) were analyzed by a flame photometer (ELICO CL354); calcium (Ca) and magnesium (Mg) were determined titrimetrically using EDTA standard solution. Bicarbonate (HCO_3) was estimated by titration with

H_2SO_4 standard solution. Chloride (Cl) was determined by titrating against AgNO_3 standard solution and sulfate (SO_4) using spectrophotometer (ELICO SL 164). Nitrate and fluoride were determined using a spectrophotometer (Shimadzu UV-1800). The analytical accuracy for the measurements of ions was resolved by calculating the ionic balance error that varied between 5 and 10% (Domenico and Schwartz 1998).

Geophysical field survey

The electrical geophysical prospecting technique consists of determining the distribution of a physical parameter which is characteristic of the subsoil on the basis of apparent resistivity made from the ground surface (Telford et al. 1990; Store et al. 2000). Twenty-five locations conducted vertical electrical sounding (VES) in the entire study area using Schlumberger array method at the maximum spreading of 220-m interval spacing electrode. Schlumberger configuration has been employed with Aquameter CRM500 (Anvic System). Curve matching technique has been used for interpretation of field data using standard master curves (Mooney and Orellana 1966; Zohdy 1969; Rajkwaterstaat 1975) as well as 'IPI2win' software through computer. The results of interpreted VES reveal three to five subsurface geoelectrical layers using Narendra and Tata (2007) interpretation method. The IPI2win software has been successfully used for making geoelectrical cross sections of the study area.

Results and discussion

Groundwater quality analysis

The statistical results were carried out using 50 groundwater samples analyzed during pre-monsoon (June 2012) and post-monsoon (January 2013) seasons which are provided

Table 1 Groundwater quality parameter statistics for various seasons

Parameter	Pre-monsoon—June 2012				Post-monsoon—January 2013			
	Minimum	Maximum	Mean	SD	Minimum	Maximum	Mean	SD
pH	6.88	8.2	7.99	0.43	6.88	8.2	7.72	0.44
EC ($\mu\text{S}/\text{cm}$)	219	9180	1077	1523.15	200	9150	1414.16	1329.97
TDS (mg/l)	140	5875	723	948.59	128	5856	859.4	827.91
Ca (mg/l)	11	536	56	80.21	20	312	71.38	47.22
Mg (mg/l)	7	209	26	39.67	8	452	39.54	63.52
Na (mg/l)	9	1205	101.5	246.13	14	1205	133.28	173.51
K (mg/l)	4	91	19.5	17.22	3	59	24.76	16.54
Cl (mg/l)	39	2964	164	446.17	35	2879	270.6	416.96
HCO_3 (mg/l)	10	1775	198	251.63	49	659	224.22	108.64
SO_4 (mg/l)	12	978	55	156.7	3	552	89.86	91.94
NO_3 (mg/l)	1	55	12	11.76	2	97	13.44	15.7
TH (mg/l)	60	2405	203.5	430.95	40	2640	269.98	360.77

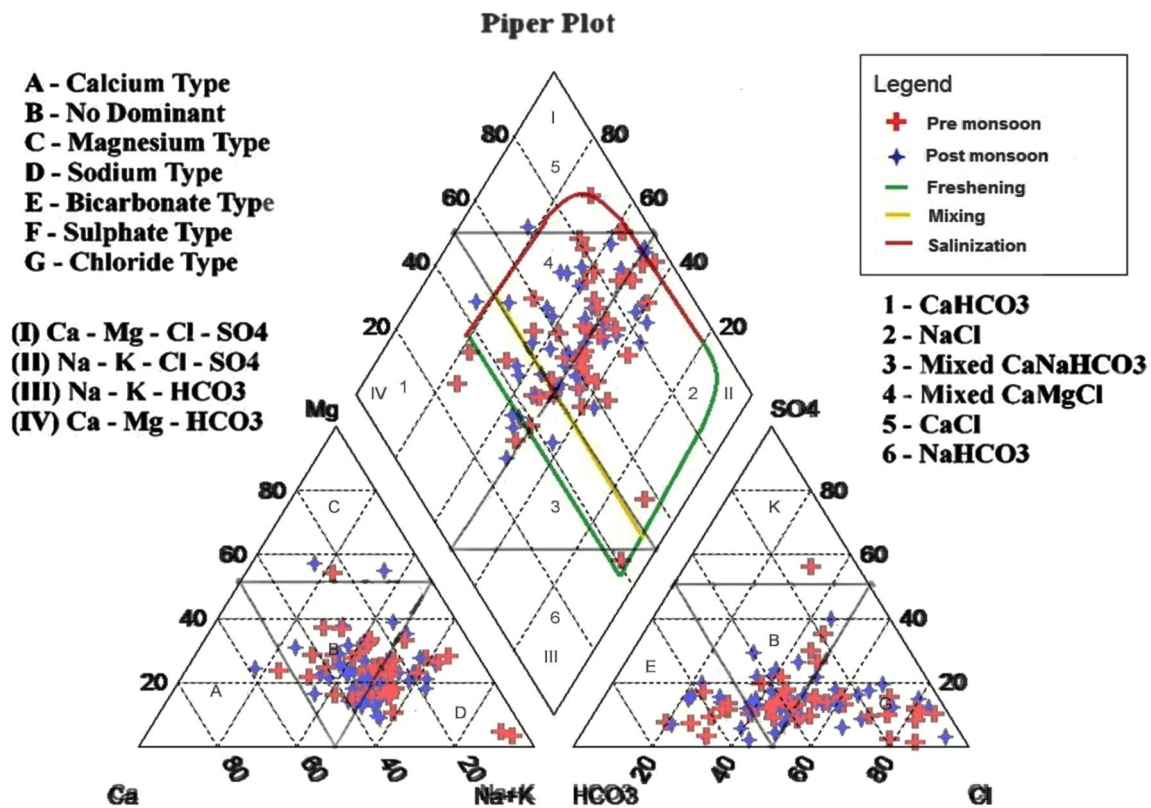


Fig. 3 Piper classification for groundwater

in Table 1. The results show that the pre-monsoon values of the majority parameters in the study area are higher absorption as compared with the post-monsoon values. The majority of samples were indicating a little alkaline environment with pH unreliable from 6.88 to 8.2. The electrical conductance of groundwater varies from 219 to 9180 $\mu\text{S}/\text{cm}$ with

an average of 1077 $\mu\text{S}/\text{cm}$ in pre-monsoon season and from 200 to 9150 $\mu\text{S}/\text{cm}$ with an average of 1414 $\mu\text{S}/\text{cm}$ for post-monsoon season.

The dominance of major ions in the samples was in the order of $\text{Na}^+ > \text{Ca}^{2+} > \text{Mg}^{2+} > \text{K}^+$ and $\text{Cl}^- > \text{HCO}_3^- > \text{SO}_4^{2-} > \text{NO}_3^-$. The maximum Na^+ concentration is higher in both seasons, i.e., 1205 mg/l. The Ca^{2+} ions of the studied samples vary between 11 and 536 mg/l with an average of 56 mg/l at the time of pre-monsoon, and increase in this value ranges from 20 to 312 mg/l with an average of 71 mg/l during the post-monsoon. The K^+ ion varied from 4 to 91 mg/l with an average value of 19.5 mg/l during the pre-monsoon and an average value of 25 mg/l in the post-monsoon. The concentration of Mg^{2+} ranges from 7 to 209 mg/l with an average of 26 mg/l during the pre-monsoon and during post-monsoon values ranges from 8 to 452 mg/l with an average value of 39.54 mg/l. Among the anionic values, Cl^- plays a major role in mineralization of the studied samples. Cl^- value ranged from 39 to 2964 mg/l with an average of 164 mg/l in the pre-monsoon time, whereas in the post-monsoon the Cl^- ion varies from 35 to 2879 mg/l with an average of 270.6 mg/l. The next dominant anion is HCO_3^- , and its concentration varies from 10 to 1775 mg/l with an average of 198 mg/l during pre-monsoon and during post-monsoon ranges from 49 to

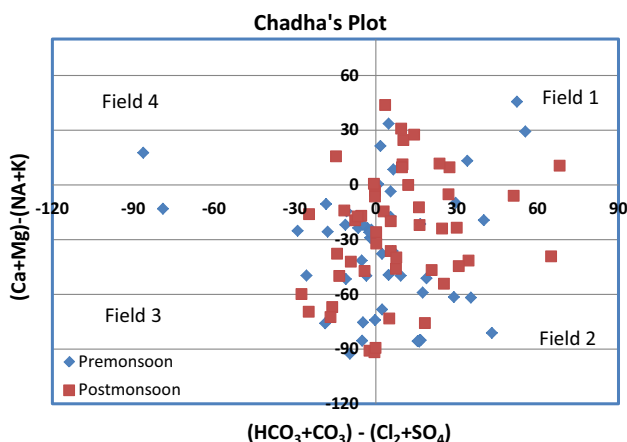
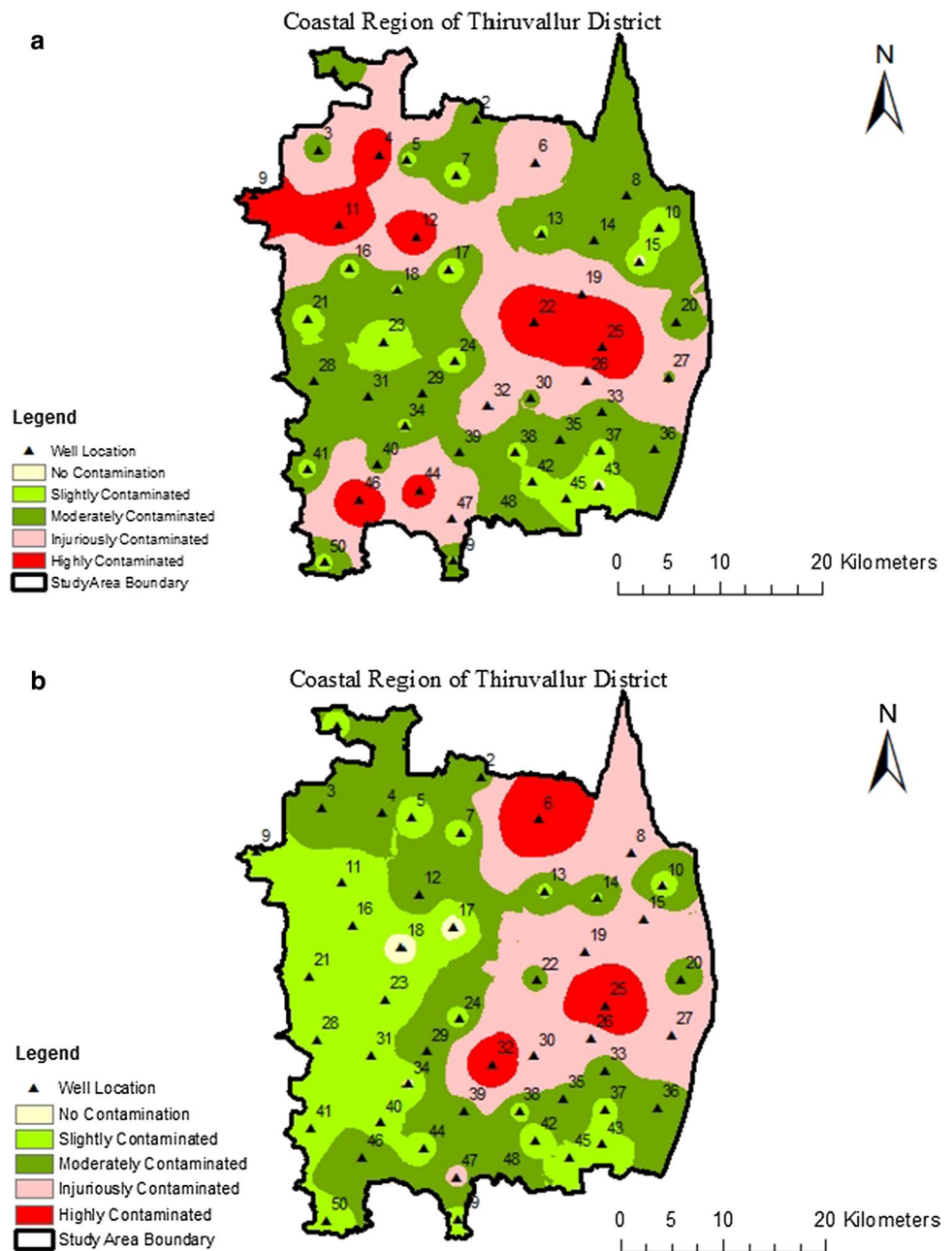


Fig. 4 Groundwater samples plotted in Chadha's plot

Fig. 5 Spatial variation map of the $Cl/CO_3 + HCO_3$ ratio during **a** pre-monsoon and **b** post-monsoon



659 mg/l with an average of 224.22 mg/l. The concentration of SO_4^{2-} ions ranges from 12 to 978 mg/l with an average of 55 mg/l in pre-monsoon and varies from 3 to 552 mg/l with an average value of 89 mg/l in post-monsoon. Nitrate concentration varies from 1 to 55 mg/l with an average of 12 and 2 to 97 mg/l with an average of 13 mg/l with reference to pre- and post-monsoon periods, respectively. The CO_3 is almost absent in all locations for both seasons. Higher TDS concentration is noticed in and around Kalpakkam, Minjur, Chinnasekkadu, Kummanur, and Thirumullaivayal locations. High values of sodium and chloride are also reported in these same locations. The presence of more TDS, sodium,

and chloride contents can be accredited to the feasibility for seawater intrusion (GurunadhaRao et al. 2011). The high concentration of TDS, sodium, and chloride in samples indicates brackishness in nature.

Piper diagram

Hydrogeochemical facies of groundwater sample were classified by Piper (1944) using a trilinear diagram. In this diagram, the triangular fields are plotted independently with milliequivalent per liter (meq/l) values of cations (Ca^{2+} , Mg^{2+}) alkali earth, ($Na^+ K^+$) alkali, (HCO_3) weak acid and

Fig. 6 Relationship of mole ratio of Cl/HCO_3 to Cl in groundwater of pre-monsoon and post-monsoon

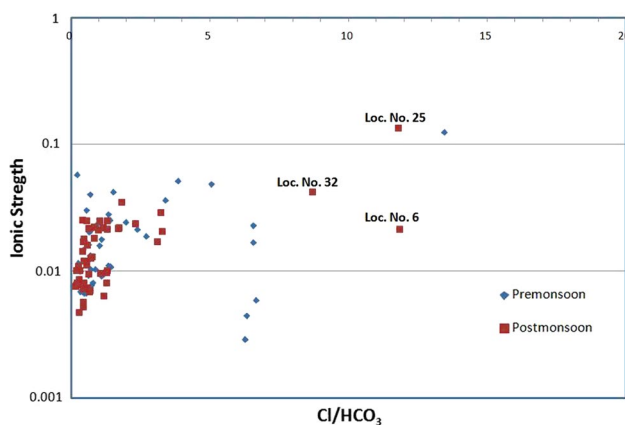
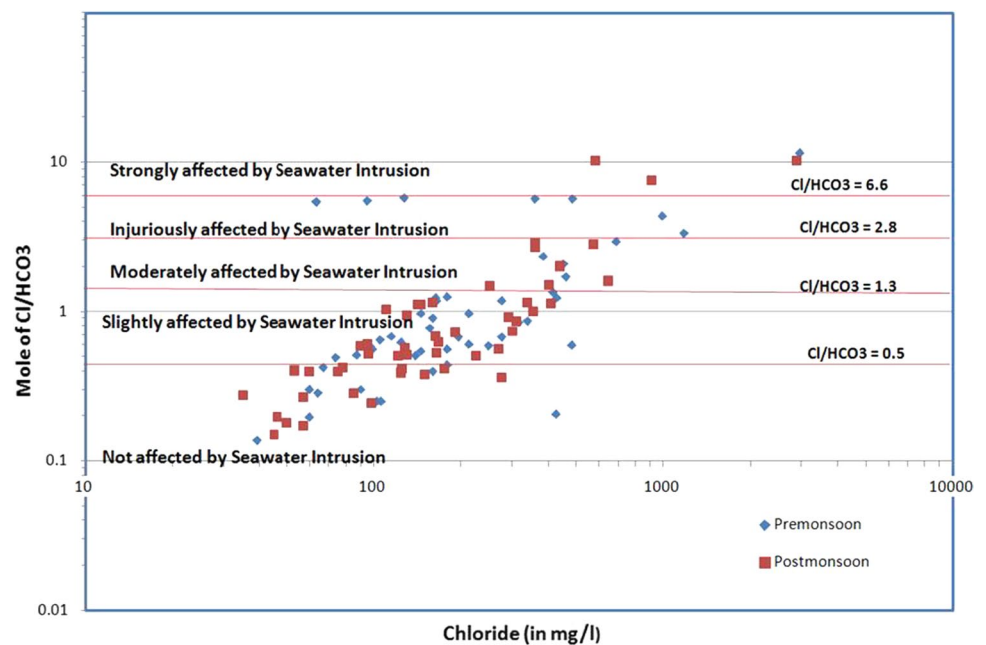


Fig. 7 Relationship between Cl/HCO_3 and ionic strength of the groundwater samples

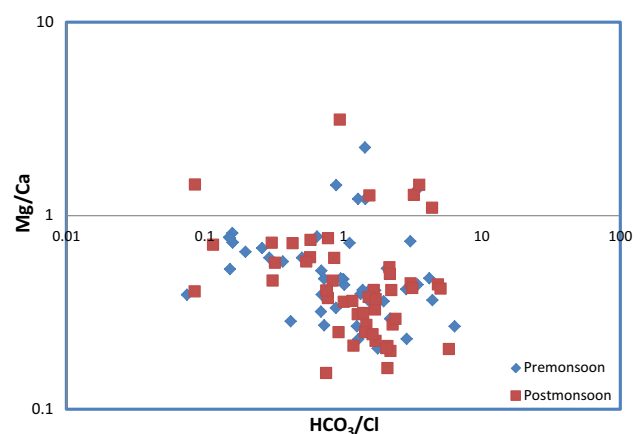


Fig. 8 Relationship between Mg/Ca and Cl/HCO_3 ratios of the groundwater sample

(SO_4^{2-} and Cl^-) strong acid. This plot has been adopted by several authors to understand the hydrogeochemical facies (Chidambaram 2000; Subramani et al. 2005; Jasrotia and Singh 2007; Prasanna et al. 2010; Sivasubramanian et al. 2013; Senthilkumar et al. 2014; Najib et al. 2017).

For recognize the chemical character of groundwater in the study area, samples have been plotted in Piper trilinear diagram (Piper 1944) using Aqua CHEM software (Fig. 3). The samples are classified as various chemical facies on the Piper diagram for both pre-monsoon of 2012 and post-monsoon period. Major types of groundwater in the study area are in the order of $\text{NaCl} > \text{mixed CaMgCl} > \text{CaHCO}_3 > \text{CaNaHCO}_3$. However, the majority of the samples are gathering in NaCl and CaMgCl field. Water types such as (mixed CaHCO_3 , mixed CaMgCl and NaCl) broadly avail in the

study region during both seasons and imply the mixing of high-salinity water caused from surface infectivity sources such as domestic wastewater, irrigation return flow and septic tank effluents with water followed by ion exchange reactions. The NaHCO_3 and CaHCO_3 water types represent the process involve mineral dissolution is representing the rock–water interaction facies in the Piper plot (Gopinath et al. 2019). The samples representing Na-Cl and mixed CaMgCl types in both seasons are identified as seawater intrusion facies present along the coastal part of the study area. The maximum Cl concentration of high saline water (Na-Cl type) is 2964 mg/l present in the coastal part. From the Piper diagram, the general trend of groundwater

chemical composition shows from mixed Ca–Mg–Cl waters to Na–Cl waters from inland toward the coast.

Chadha's plots

In this study, Chadha 1999 hydrochemical diagram was used to understand the hydrochemical reactions involved in the study area. This method was successfully applied by many researchers in coastal aquifers to resolve the evolution of two diverse hydrogeochemical processes like seawater intrusion and rock–water interaction (Vandenbohede et al. 2010; Thilagavathi et al. 2012; Senthilkumar et al. 2017a, b).

As shown in the Chadha's plot (Fig. 4), 42% of the samples fall at in Field 3 (Na–Cl) during the pre-monsoon season, suggesting that the waters are distinctive seawater mixing and are typically constrained to the coastal areas reveal that the sea water intrusion facies of this region. The 20% of post-monsoon samples fall in Field 1 which is recharging water type. The 32% of the samples during both seasons drop at Field 2 (reverse ion exchange field), enlightening that the waters are represented groundwater where Ca + Mg is in excess to Na + K either due to the superior release of Ca and Mg from mineral weathering

of uncovered bedrock reveal that the rock–water interaction facies of the study area. Only 2% of samples fall in Field 4; it is (Na–HCO₃) type of waters, not as much of importance in this area during both seasons.

Cl/CO₃ + HCO₃ ratio

The spatial distribution map of Cl/HCO₃ + CO₃ ratio has been prepared for both pre-monsoon and post-monsoon periods (Fig. 5a, b). Cl/HCO₃ + CO₃ ratios range between 0.3 and 23.2, and it reveals the strong constructive linear relation with Cl ion concentrations (Fig. 6). This linear relationship indicates mixing of fresh groundwater with sea waters. In view of the Cl concentration (35 mg/l) values and the ratio of Cl/HCO₃ + CO₃, 26% of the groundwater was strongly affected by the saline water and 74% were slightly affected during pre-monsoon season. During the post-monsoon period, 20% of the samples is strongly affected by saline water intrusion and the remaining samples are slightly to moderately contaminated. The high ratio in groundwater around Rakkampalayam, Minjur and Kummanur (Loc. No. 6, 25 and 32) during the post-monsoon period may be due

Table 2 Layer-wise geoelectrical parameters of the coastal region of Thiruvallur district

VES. no.	VES location	Resistivity (Ω m)					Thickness (m)			
		ρ_1	ρ_2	ρ_3	ρ_4	ρ_5	h_1	h_2	h_3	h_4
1	Elavur	1399.0	7.8	120.0	6.2	–	0.8	1.4	0.8	–
2	Madarpakkam	583.0	178.0	213.0	6.5	–	1.0	4.3	0.4	–
3	Rettambedu	17.4	7.1	25.2	0.1	–	0.2	19.1	13.8	–
4	Kolur	3.5	22.7	2.1	5.2	–	0.3	0.2	0.5	–
5	Gummudipoondi	10,713.0	15.1	127.0	16.9	–	0.4	0.5	0.5	–
6	Andarmadam	18.8	2.0	10.4	0.0	–	0.2	0.9	0.3	–
7	Vanjivakkam	3.3	1.0	3.0	23.9	–	1.0	6.5	34.5	–
8	Medur	16.0	2.7	91.3	6.5	–	0.5	0.8	0.6	–
9	Kavarapettai	5.6	6.2	4.0	11.0	–	0.8	0.3	5.3	–
10	ChinnaManopuram	9.3	28.2	0.6	5.7	–	0.3	0.8	0.3	–
11	Arani	1073.0	8.6	418.0	8.2	–	0.4	0.4	1.0	–
12	Vayalur	26.4	4.0	111.0	2.6	–	2.6	1.6	2.5	–
13	Chinnambedu	5.6	1.6	265.0	10.9	–	1.0	0.4	0.7	–
14	Krishnapuram	316.0	3851.0	15.0	6.5	–	0.4	0.6	47.0	–
15	Kanniyambakkam	15.6	5.2	23.0	4.4	–	1.1	0.7	0.7	–
16	Eliyambedu	97.8	2.1	36.2	12.3	–	0.6	0.4	0.9	–
17	Minjur	4.1	15.1	3.5	51.5	–	0.3	0.5	90.2	–
18	Kannigaippper	7.5	1.3	41.8	7.2	–	1.9	0.4	3.0	–
19	Agaram	8.0	1.6	74.2	7.5	–	1.3	1.8	2.8	–
20	Kottakuppam	13.9	6.0	1.2	8.0	–	0.7	0.2	0.3	–
21	Vallur	1.2	3.7	2.4	14.9	–	2.4	16.4	10.2	–
22	Agaram	5.2	424.0	13.9	0.0	–	1.6	1.8	0.0	–
23	Cholavaram	21.1	1.7	12.8	0.0	–	0.7	0.4	0.0	–
24	Andarkuppam	0.2	25.8	0.2	1.5	–	0.1	0.3	1.2	–
25	Madhavaram	4.7	106.0	12.9	1.7	11.5	0.2	0.6	0.7	1.6

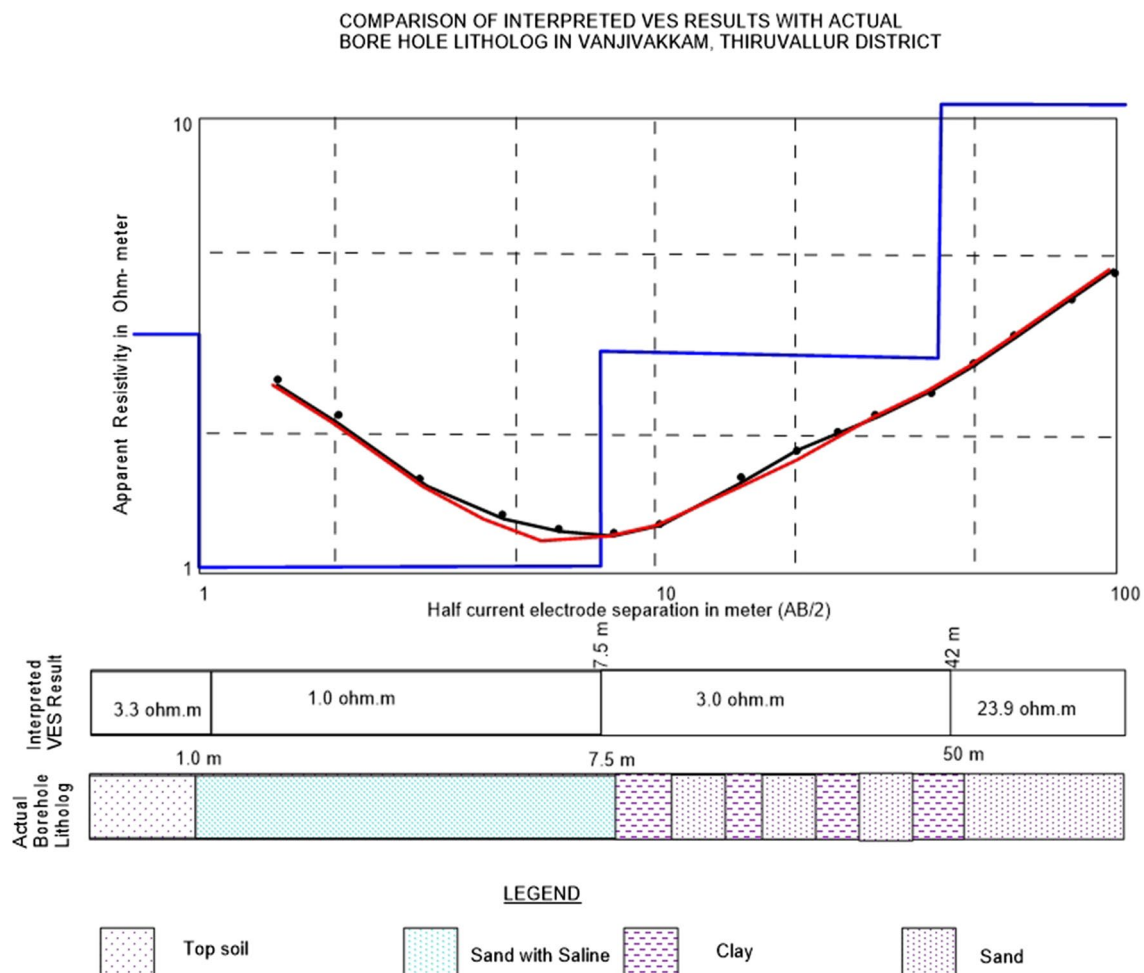


Fig. 9 VES results and borehole lithology calibration in the study area (VES location No.7)

to the upcoming of saline water, which may be due to over-exploitation of groundwater.

Cl/HCO₃ versus ionic strength

The relations of Cl/HCO₃ ratio to ionic strength of the samples (Fig. 7) show the most of the samples have a linear trend to the ionic strength (IS). The inaccurate value of ionic strength (IS) can also be computed from the specific conductance of the solution by Lind (1970). If the composition is indefinite for water with a specific conductance of 1000 $\mu\text{S}/\text{cm}$, the calculated value of IS could range from 0.0085 to 0.027. The linear increase of Cl/HCO₃ ratio with IS indirectly indicates the saline water incursion into the aquifer. The IS values and the ratio are lesser in the pre-monsoon samples than those of the post-monsoon sample. During the post-monsoon season, samples show higher IS in the location of Rakkampalayam, Minjur, and Kummanur (Loc. No. 6, 25 and 32) which may be due to backwater flow during the post-monsoon period of this area. Hence, it is evident that the saline intrusion is more important in the study area during the post-monsoon.

Table 3 Resistivity range of lithological units. (Source: Arulprakasam 2010)

Sl. no.	Resistivity ranges in Ωm	Formation
1	Less than 3	Saline formation
2	3–5	Clay
3	5–12	Sandy clay
4	12–50	Sand
5	50–150	Sandstone/limestone
6	150–250	Weathered rock
7	250–500	Fractured rock
8	500–1000	Semi fractured rock
9	More than 1000	Massive crystalline rock

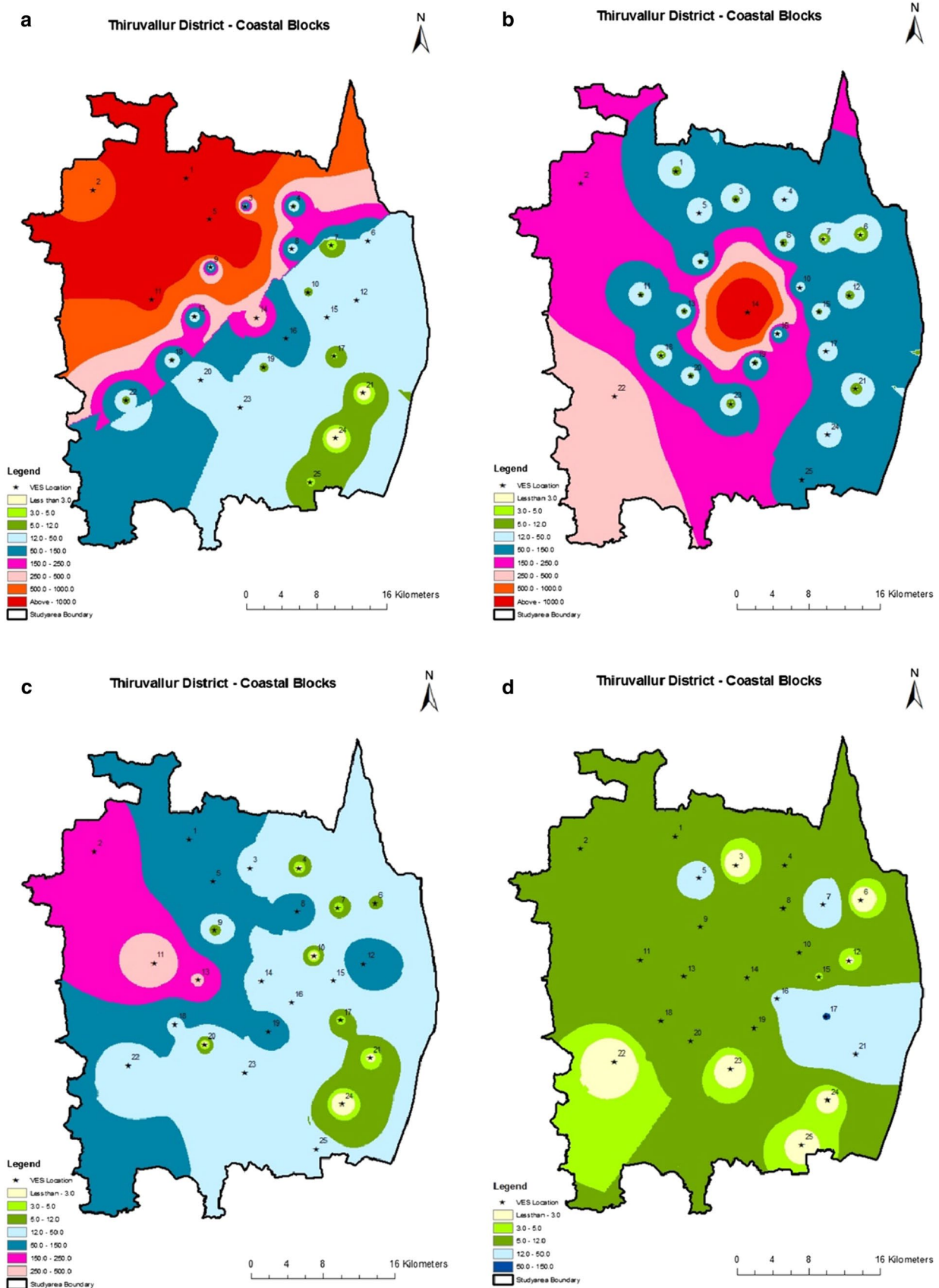


Fig. 10 a First-layer resistivity. b Second-layer resistivity. c Third-layer resistivity. d Fifth-layer resistivity

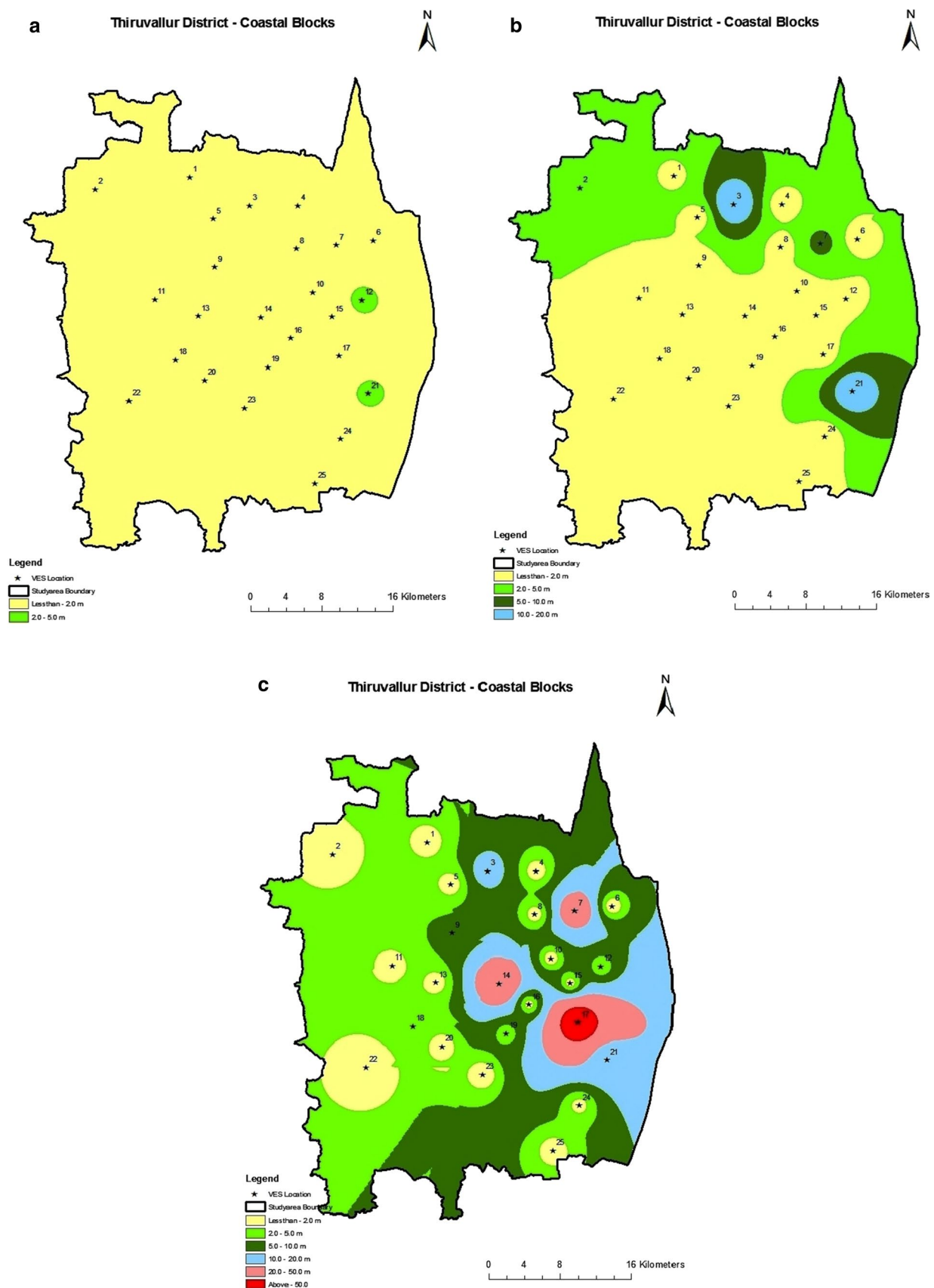


Fig. 11 **a** First-layer thickness in meter. **b** Second-layer thickness in meter. **c** Third-layer thickness in meter

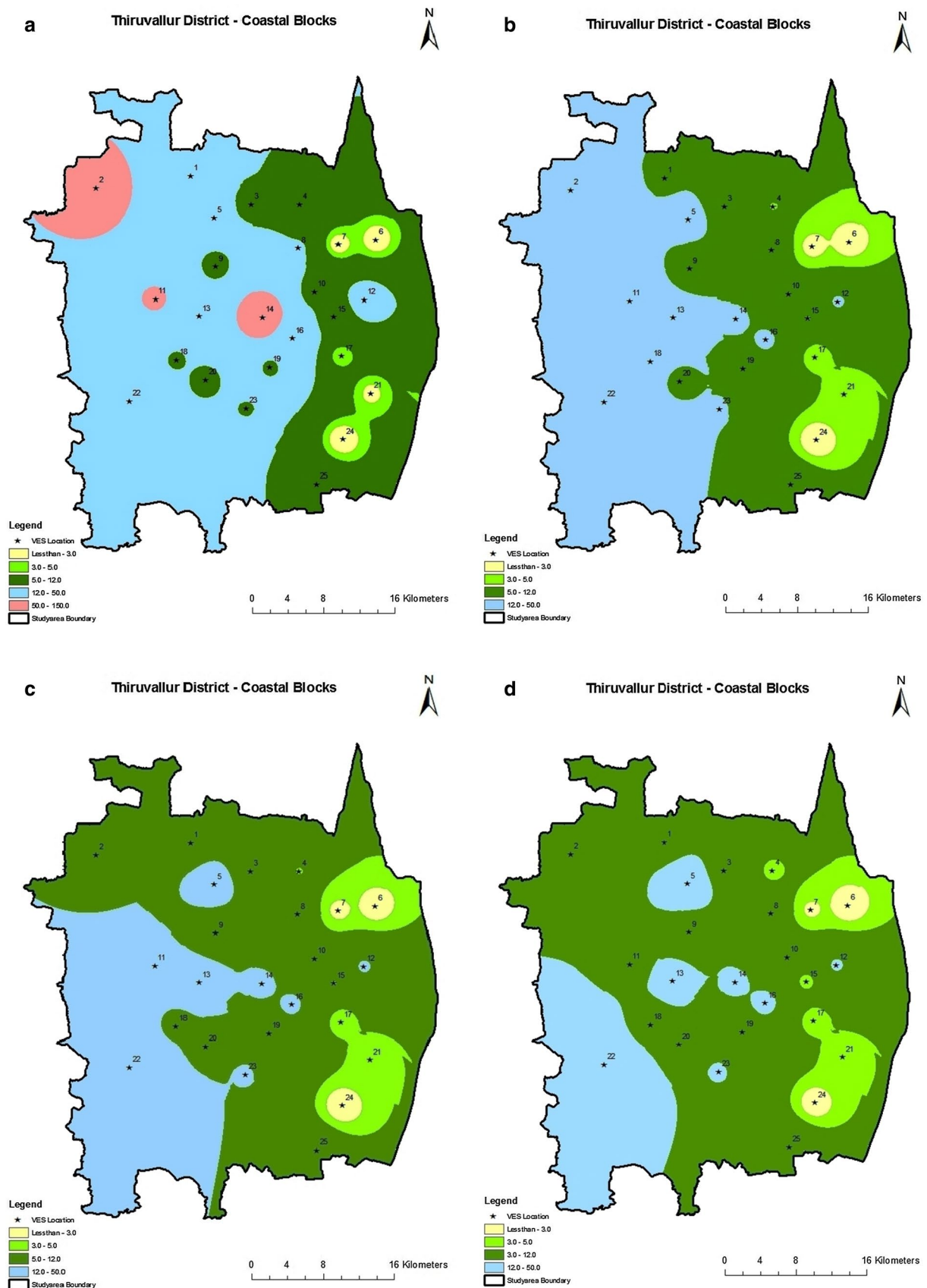


Fig. 12 Iso-apparent resistivity map at **a** 10 m, **b** 20 m, **c** 30 m, **d** 40 m, **e** 50 m depth

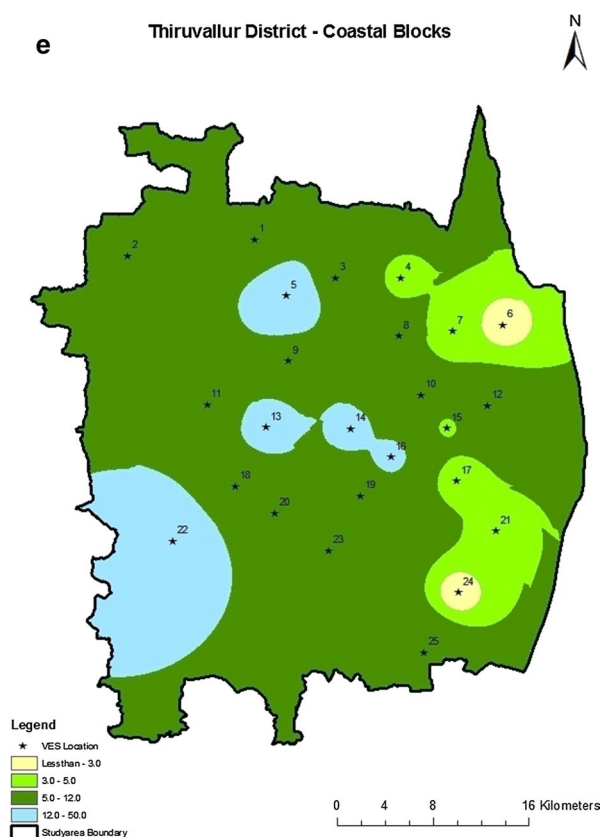


Fig. 12 (continued)

Mg^{2+}/Ca^{2+} and Cl^{-}/HCO_3^{-} ratios

The Mg^{2+}/Ca^{2+} ratio can be projected as an indicator for delineating the seawater–freshwater interface. Mondal et al. (2008) observed that very low HCO_3^{-}/Cl^{-} and uneven high Mg^{2+}/Ca^{2+} (molar ratios) indicate the alteration of fresh water to saline water in coastal aquifers. The study of these ratios in the samples of the study area (Fig. 8) indicates a value of Mg/Ca between 0.1 and 1 which points out a high concentration of Ca, and some wells indicate a ratio superior to 1 indicating a high concentration of Mg ion. The post-monsoon groundwater samples have higher Mg^{2+} values compared to that of the Ca^{2+} which has an indirect behavior of the seawater intrusion.

Geoelectrical resistivity survey

In the groundwater investigation survey, geoelectrical resistivity studies have wide applications (Arora 1986; Ilkisik et al. 1997; Yadav and Abolfazli 1998). The Schlumberger vertical electrical sounding (VES) study, carried out in the coastal part of Thiruvallur area, aimed to delineate the freshwater and seawater interface using

GIS platform. Sounding data may be interpreted in both qualitative and quantitative manner. In qualitative analysis, the most important factor is the shape of the VES curve, from which it is possible to decipher the number of layers and their resistivity contact. When the data of several stations are available, they can be interpreted by depicting in maps, the areal distribution of the types and sounding curves and apparent resistivity (Karanth 1987). Quantitative interpretation of sounding curves can be done by analytical and empirical methods. Initially, curve matching techniques are commonly adopted in the analytical method. The observed sounding curve is plotted on the same modulus as that of the speculative master curves of apparent resistivity versus electrode spacing, for different combinations of thicknesses and resistivity (Mooney and Wetzell 1956; Orellana and Mooney 1966; Ghosh 1971 and Zohdy 1974).

The IPI2win software developed by Moscow State University has been used for interpretation by which resistivity of different layers is estimated. Once the resistivity and thicknesses of different layers are known, the data may be used to prepare a geoelectrical section of the VES spot. The interpreted results of vertical electrical soundings in terms of resistivity (ρ_a) and thickness (h) of various layers deciphered are given in Table 2. The RMS error found varies from 2.38 to 12.6% in the inverse model resistivity sections. Comparison of VES results with actual borehole lithology at a few sites like Vanjivakkam (Loc No. 7) by Arulprakasam (2017) is shown in Fig. 9. Moreover, the VES sounding curve resistivity has been calibrated with geological lithology of Vanjivakkam location. In general, the resistivity of sand with saline water formation is shown to $> 3 \Omega m$ for first and second layers. The third layer encountered in 7.5 to 52 m with sandy clay formation shows 3 to 15 Ωm resistivity, respectively. The fourth layer resistivity after 42 m is observed sand formation with the resistivity of 12 to 50 Ωm .

Layer resistivity

Iso-resistivity contours maps were drawn for four layers based on the interpreted VES statistics proven in Table 3. In the study area, the primary layer (Fig. 10 a) resistivity varies from 0.2 to 10,713 Ωm . The low resistivity ($< 3 \Omega m$) is noticed in southeastern part which may be due to sand with saline water. The high resistivity ($> 500 \Omega m$) is visible in north and northwestern parts of the look at the place; this may be due to laterite formation. The resistivity range of 12–50 Ωm is visible in middle a part of the study place; this may be because of the presence of sand formation and also seawater intrusion (Fadili et al. 2017). For the contaminated formation due to seawater, the resistivity ranges between 8 and 50 Ωm (Fadili et al. 2017; Senthilkumar et al. 2017a,

Table 4 Aquifer geoelectrical properties of the coastal region of Thiruvallur district

VES. no.	VES location	Transverse resistance (T) m^2	Longitudinal conductance (S) mhos	Thickness (h) in meter
1	Elavur	1226.12	0.19	3
2	Madarpakkam	1433.6	0.03	5.70
3	Rettambedu	486.85	3.25	33.10
4	Kolur	6.64	0.33	1.00
5	Gummudipoondi	4356.25	0.04	1.40
6	Andarmadam	8.68	0.49	1.40
7	Vanjivakkam	113.3	18.30	42.00
8	Medur	64.94	0.33	1.90
9	Kavarapettai	27.54	1.52	6.40
10	ChinnaManopuram	25.53	0.56	1.40
11	Arani	850.64	0.05	1.80
12	Vayalur	352.54	0.52	6.70
13	Chinnambedu	191.74	0.43	2.10
14	Krishnapuram	3142	3.13	48.00
15	Kanniyambakkam	36.9	0.24	2.50
16	Eliyambedu	92.1	0.22	1.90
17	Minjur	324.48	25.88	91.00
18	Kannigaipper	140.17	0.63	5.30
19	Agaram	221.04	1.33	5.90
20	Kottakuppam	11.29	0.33	1.20
21	Vallur	88.04	10.68	29.00
22	Agaram	771.52	0.31	3.40
23	Cholavaram	15.45	0.27	1.10
24	Andarkuppam	8	6.51	1.60
25	Madhavaram	76.29	1.04	3.10

b). The resistivity of the pinnacle layer is in comparison with the geology of the observed location which confirms the presence of above-cited formations. The iso-resistivity values of second layer range from 1 to 3851 Ωm (Fig. 10b). The low resistivity ($< 3 \Omega m$) is present as small patches in a coastal tract of the study area which are may be due to sand with saline water. The high resistivity zones ($> 1000 \Omega m$) are visible in the central part of the study area indicating a very critical position of groundwater availability due to the presence of dry sands in this region. The resistivity ranging between 250 and 500 Ωm occupies southwestern part of the study area which confirms the occurrence of the sandstone formation.

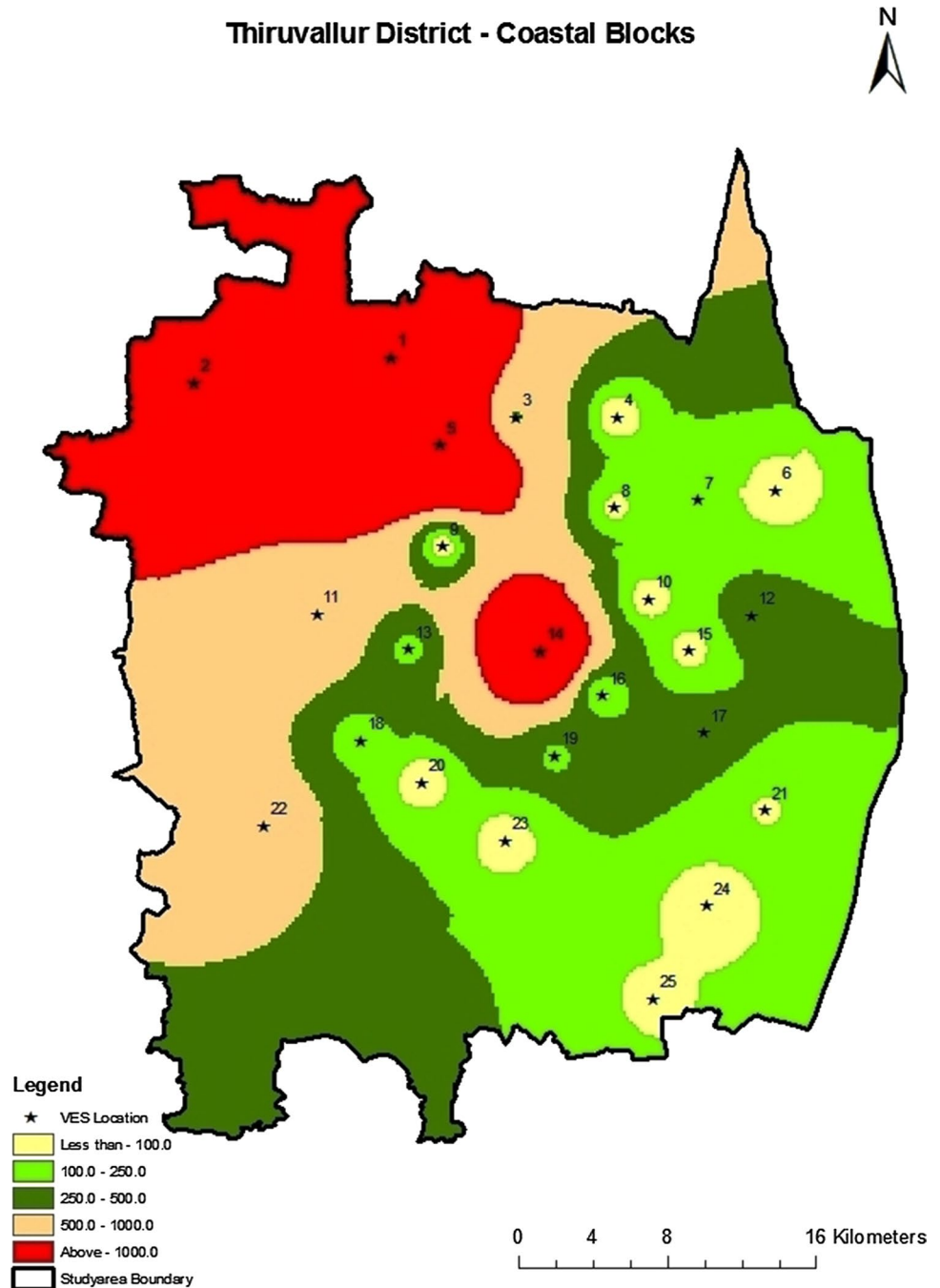
The iso-resistivity of the third layer ranges from 0.2 to 418 Ωm (Fig. 10c). The low-resistivity area ($< 3 \Omega m$) occupied as patches in coastal areas of the take a look at region indicating the presence of saline water. The resistivity ranging from 12 to 50 Ωm shows thick sand formation in an important part of the study location. The resistivity values greater than 150 Ωm are determined in northwestern component confirming the life of compact lateritic formation. The

resistivity values lightly lower toward the central and eastern parts of the observed area are because of the presence of alluvium. The fourth layer iso-resistivity of the look at area ranges from 0.00 to 51.5 Ωm (Fig. 10d). The low resistivity is seen as pockets in southern and eastern parts indicating the prevalence of saline water in this place. Relaxation of the place is characterized via the resistivity values ranging from 5 to 12 which implicate sandy clay formation. The thickness of the individual layer of all 25 VES locations is delineated from the VES curve (h_1 , h_2 , h_3) and shown in Table 3. The spatial distributions of the thickness of first, second and third layers of the study place are shown in Figs. 11a–c, respectively. The thickness of the first layer varies from 0.1 to 2.6 m. Maximum thickness of the second layer is 19.1 m, and its minimal thickness is 0.2 m. The third layer has its thickness from 0.3 to 90.2 m.

Iso-apparent resistivity

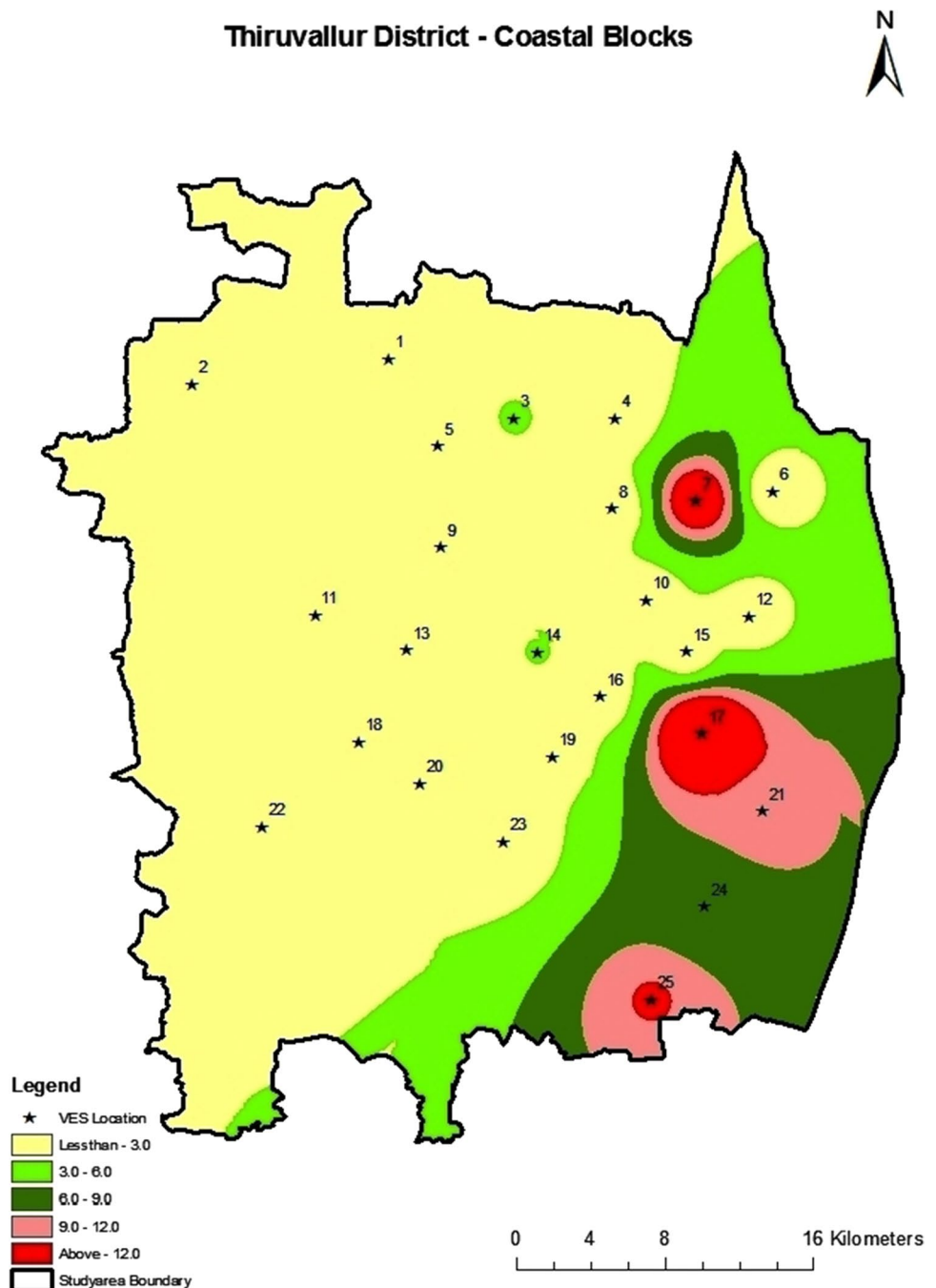
Apparent resistivity thematic maps have been prepared at different depth levels of 10, 20, 30, 40 and 50 m for all 25

Fig. 13 Transverse resistance (*T*) map



VES locations using ArcGIS platform in IDW interpolation method to examine the difference in resistivity at the particular depths due to subsurface anisotropy. Resistivity contours for various depths quite symbolize the subsurface lithological difference under the obtainable hydrological conditions (Fig. 12). Resistivity contours for 10-m depth levels show mostly low resistivity values ($< 50 \Omega\text{m}$) of the topsoil collected of alluvial sediments, laterite, silty clay, and clay (Fig. 12a). At the depth of 20, 30, 40, 50 m, the counters are

generally in the range of 5 to $50 \Omega\text{m}$ (Fig. 12b–e). From the iso-resistivity thematic maps, it is concluded that resistivity $< 10 \Omega\text{m}$ indicates the presence of saline water. Regions having low iso-apparent resistivity (i.e., $< 10 \Omega\text{m}$) occur along the southern coastal tract extending up to central portion which clearly confirms the presence of saline water at various depths below the ground level. Freshwater occupies a major portion along the northern part and is seen in pockets in the central part of the study area.

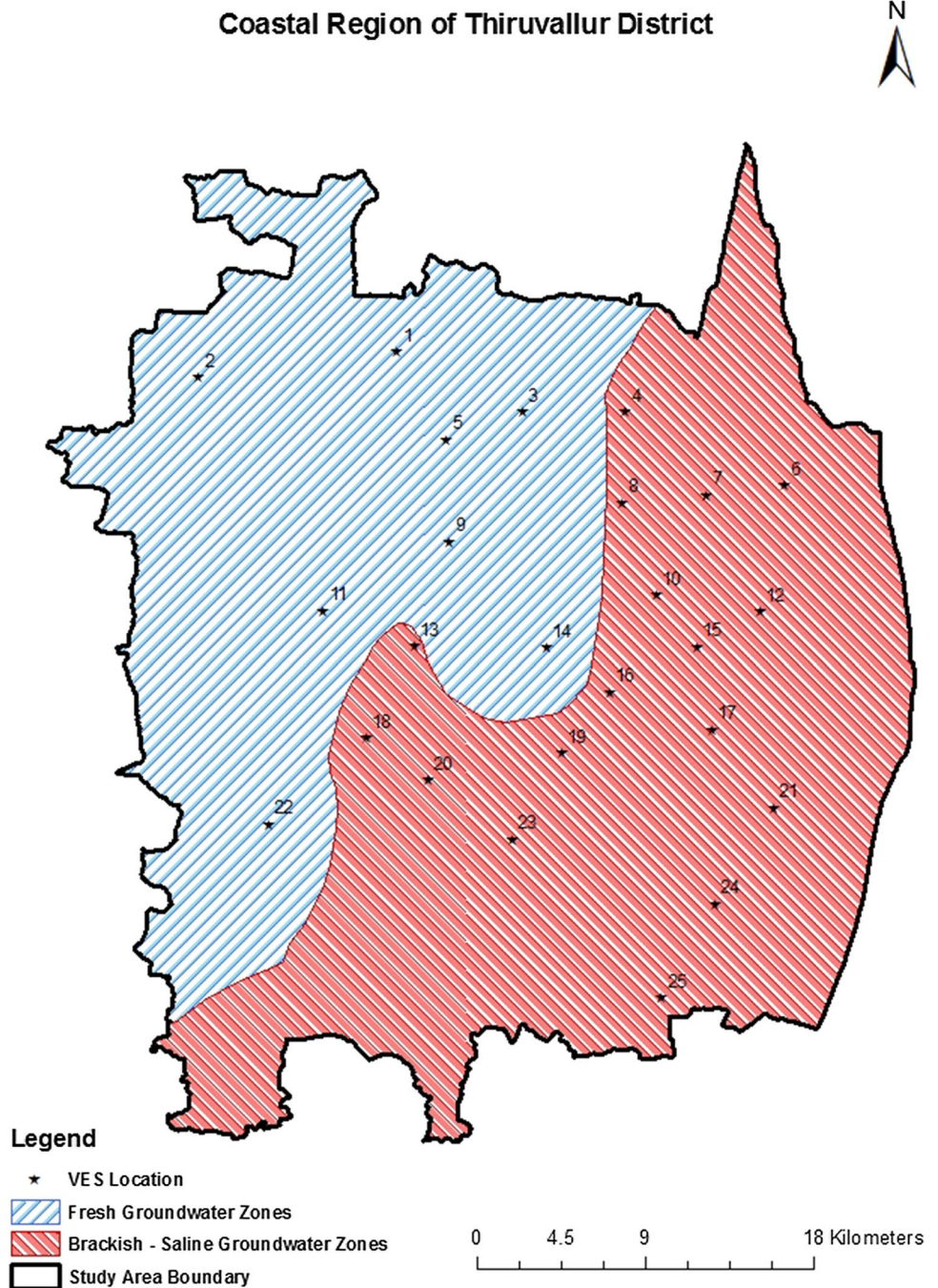
Fig. 14 Longitudinal conductance (S) map

Geoelectrical parameter

A geologic section differs from a geoelectrical phase while the limits between geologic layers do no longer coincide with the limits between layers characterized with the aid of different resistivity values. Therefore, the electrical boundaries keeping apart layers of different resistivity values may also or may not coincide with limitations keeping apart layers of various geologic age or one of lithologic composition. As

mentioned in advance, a geoelectrical layer is defined with the aid of two essential parameters together with layer resistivity (ρ) and its thickness (h). Geoelectrical parameters such as formation resistivity, overall longitudinal conductance, and intensity to the bedrocks are useful guides, in evaluating the groundwater capacity of a site (Ballukarya 2001). A few important geoelectrical parameters which can be derived from the layer resistivity and their thickness are (1) transverse resistance (T) and longitudinal conductance (S).

Fig. 15 Final overlay map for fresh-brackish water zone of the area



Transverse resistance

The transverse resistance (T) and longitudinal conductance (S) values are successfully useful for demarcating ground-water potential (Narendra and Rajendra Prasad 2009). Singh (2003) stated that the transverse resistance (T) and longitudinal conductance (S) are used for better declaration of thin layers of both resistive and conductive properties.

The transverse resistance (T) values can be intended from VES results by using the following equation.

$$T = \sum_{i=1}^n h_1 \times \rho_1 + h_2 \times \rho_2 \cdots + h_n \times \rho_n (\Omega\text{m}^2)$$

According to Zohdy (1974), increase in T values suggests an increase in the thickness of the resistive cloth. Higher-aquifer transmissivity zones can be positioned by way of better T value. Arulprakasam (2010) stated that the better (T) and (S) values indicating a very good ability, however, brackish to saline nature and deeper basement. In the

present study, the transverse resistance values of the study area vary from 6.64 to 4356.25 Ωm^2 with a median value of 678.48 Ωm^2 (Table 4). The spatial distribution of T values of the take a look at area shown in Fig. 13 exhibited high values ($> 1000 \Omega\text{m}^2$) in the western part of the observation area and low values ($< 500 \Omega\text{m}^2$) within the eastern and southern components.

Longitudinal conductance

The longitudinal conductance (S) values are derived from VES results for the present study area using by the following equation.

$$S = \sum_{i=1}^n \frac{h_i}{\rho_i} + \frac{h_2}{\rho_2} \dots + \frac{h_n}{\rho_n} \text{ (mhos)}$$

The S values of the take a look at the area are given in Table 4. Variation within the overall thickness of low-resistivity cloth can be efficaciously diagnosed by means of the use of the distinction in s from one intensity probing station to the other (Zohdy 1969; Henriet 1975; Worthington 1977 and Galin 1979). In the observe region, longitudinal conductance (S) values vary from 0.03 to 25.88 mhos with a mean value of 3.88 mhos (Fig. 14). Longitudinal conductance ranging above common happens alongside the coastal tract indicating the presence of marine sediments in this area. The low ' S ' values seen around the north and northwestern parts are observed which coincides with the alluvium formations. Very high ' S ' values (above 12 mhos) arise at Vanjivakkam, Minjur, and Madhavaram (Loc. Nos. 7, 17 & 25) which shows the presence of saline water and clay-dominated regions. The high ' T ' and occasional ' S ' values in northwestern part of the study place indicate the presence of sparkling groundwater zone. The excessive ' T ' and low ' S ' values present along the coastal tract suggest brackish to saline groundwater, and the remaining location is characterized by using moderate groundwater zones shown in Fig. 15; this without a doubt indicated the brackish water sector is extending up to 35 km from the coast within the south part and its width is narrowly reduced toward the northern part of the take a look at area that is up to 15 km from the coast. Southern part of the study place is broadly extending to brackish water region particularly because of the over-extraction of groundwater via Chennai metropolis.

Conclusion

Integrated geochemical and geophysical techniques have been employed to assess the seawater intrusion status in the study area. The presence of seawater intrusion was reported by Central Ground Water Board in and around Minjur

area. In this geochemical study, major ionic compositions, TDS sodium and chloride concentrations effectively indicated the influence of seawater intrusion. $\text{NaCl} > \text{mixed CaMgCl} > \text{CaHCO}_3 > \text{CaNaHCO}_3$ groundwater facies were found in the study area which is clearly indicated in Piper and Chadha plots. However, most of the samples are dominated by NaCl and CaMgCl segments indicating the sea water intrusion. Various ionic ratios like $\text{Cl}/\text{CO}_3 + \text{HCO}_3$ ratio, Cl/HCO_3 versus ionic strength, $\text{Mg}^{2+}/\text{Ca}^{2+}$ and $\text{Cl}^-/\text{HCO}_3^-$ ratios also indicated the sea water intrusion infringed the following locations of Rakkampalayam, Minjur, and Kummanur. Vertical electrical sounding techniques were successfully applied to identify the seawater and brackish water zones in the study area. From the sounding results, thickness of various layers and iso-apparent resistivity are successfully delineated. Regions of low iso-apparent resistivity ($< 10 \Omega\text{m}$) occur along the southern coastal tract extending up to central portion which clearly confirms the presence of saline water at various depths below the ground level. Based on the transverse resistance (T) and longitudinal conductance (S) of the study area, the final output overlay map indicated clearly the seawater intrusion.

Open Access This article is distributed under the terms of the Creative Commons Attribution 4.0 International License (<http://creativecommons.org/licenses/by/4.0/>), which permits unrestricted use, distribution, and reproduction in any medium, provided you give appropriate credit to the original author(s) and the source, provide a link to the Creative Commons license, and indicate if changes were made.

References

- Amores MJ, Verones F, Raptis C, Juraske R, Pfister S, Stoessel F, Antón A, Castells F, Hellweg S (2013) Biodiversity impacts from salinity increase in a coastal wetland. *Environ Sci Technol* 47(12):6384–6392
- APHA (2005) Standard methods for the examination of water and wastewater, 21st edn. American Public Health Association, Washington
- Aris AZ, Abdullah MH, Ahmed A, Woong KK (2007) Controlling factors of groundwater hydrochemistry in a small island's aquifer. *Int J Environ Sci Technol* 4(1735–1472):441–450
- Arora CL (1986) Geoelectric study of some Indian geothermal areas. *Geothermics* 15(5–6):677–688
- Arulprakasam V (2010) Integrated groundwater management for sustained development of groundwater resources in Vanur Region, Tamil Nadu, India, Unpublished Ph.D. Thesis, University of Madras, Chennai
- Arulprakasam V (2017) State report on groundwater geophysics Tamil Nadu & U.T of Puducherry, Chennai
- Ballukarya PN (2001) Hydrogeophysical investigations in Namagiripettai area, Namakkal district. *J Geol Soc India* 58:239–249
- Banerjee P, Singh VS, Singh A, Prasad RK, Rangarajan R (2012) Hydrochemical analysis to evaluate the seawater ingress in a small coral island of India. *Environ Monit Assess* 184(6):3929–3942
- CAMP (2000) Integrated aquifer management plan: final report. Gaza coastal aquifer management program. Metcalf and Eddy Inc. in

- cooperation with the Palestinian Water Authority (PWA), s.l.: United States Agency for International Development, USAID. Contract No. 294-C-00-99-00038-00
- CGWB (2007) Central ground water board's district groundwater brochure. Tiruvallur district, Tamil Nadu
- Chadha DK (1999) A proposed new diagram for geochemical classification of natural waters and interpretation of chemical data. *Hydrogeol J* 7(5):431–439
- Chidambaram S (2000) Hydrogeochemical studies in and around Neyveli mining region, Tamilnadu, India. Ph.D., Thesis, Department of Earth Sciences, Annamalai University
- Choudhury K, Saha D, Chakraborty P (2001) Geophysical study for saline water intrusion in coastal alluvial terrain. *J Appl Geophys* 46:189–200
- Davis SN, Whittemore DO, Fabryka-Martin J (1996) Uses of chloride/bromide ratios in studies of potable water. *Ground Water* 36(2):338–350
- Domenico PA, Schwartz W (1998) Physical and chemical hydrogeology, 2nd edn. Wiley, New York, p 506
- Fadili A, Najib S, Mehdi K, Riss J, Malaurent P, Makan A (2017) Geoelectrical and hydrochemical study for the assessment of seawater intrusion evolution in coastal aquifers of Oualidia, Morocco. *J Appl Geophys* 146:178–187
- FAO (1997) Seawater intrusion in coastal aquifers, guidelines for study, monitoring and control. Water report no 11
- Frohlich RK, Urish DW, Fuller J, Reilly MO (1994) Use of geoelectrical method in groundwater pollution surveys in a coastal environment. *J Appl Geophys* 32:139–154
- Galin DL (1979) Use of longitudinal Conductance in vertical electrical sounding—induced potential method for solving hydrogeologic problems. *Vestik Mosk Univ Geol* 34(3):97–100
- Ghosh DP (1971) Inverse filter coefficient for the computation of apparent resistivity: standard curves for a horizontally stratified earth. *Geophys Prospect* 19(4):769–775
- Giménez-Forcada E (2010) Dynamic of sea water interface using hydrochemical facies evolution diagram. *Groundwater* 48(2):212–216
- Giménez-Forcada E (2014) Space/time development of seawater intrusion: a study case in Vinaroz coastal plain (Eastern Spain) using HFE-Diagram, and spatial distribution of hydrochemical facies. *J Hydrol* 517:617–627
- Gnanasundar D, Elango L (1999) Groundwater quality assessment of a coastal aquifer using geoelectrical techniques. *J Environ Hydrol* 7(2):21–33
- Gopinath S, Srinivasamoorthy K, Saravanan K, Prakash R, Karunanidhi D (2019) Characterizing groundwater quality and seawater intrusion in coastal aquifers of Nagapattinam and Karaikal, South India using hydrogeochemistry and modeling techniques. *Hum Ecol Risk Assess Int J*. <https://doi.org/10.1080/10807039.2019.1578947>
- Gowtham B (2003) Integrated hydrogeological investigations of lower Gundar Basin, Tamil Nadu, India, Unpublished Ph.D Thesis, University Of Madras, Chennai
- GSI (2005) District resource map, Thiruvallur and Chennai district, Tamil Nadu, published by Geological Survey of India
- GurunadhaRao VVS, TammaRao G, Surinaidu L, Rajesh R, Mahesh J (2011) Geophysical and geochemical approach for seawater intrusion assessment in the Godavari Delta Basin, A.P., India. *Water Air Soil Pollut* 217:503–514. <https://doi.org/10.1007/s11270-010-0604-9>
- Henriet JP (1975) Direct interpretation of the Darzarrouk parameters in groundwater surveys. *Geophys Prosp* 24:344p
- Hodlur GK, Dhakate R, Sirisha T, Panaskar DB (2010) Resolution of freshwater and saline water aquifers by composite geophysical data analysis methods. *Hydrol Sci J* 55(3):414–434
- Ilkisik OM, Gurer A, Tokgoz T, Kaya C (1997) Geoelectromagnetic and geothermic investigations in the Ihlara valley geothermal field. *J Volcanol Geotherm Res* 78:297–308
- Jasrotia AS, Singh Rajinder (2007) Hydrochemistry and groundwater quality, around Devak and Rui watersheds of Jammu region, Jammu and Kashmir. *J Geol Soc India* 69(5):1042–1054
- Karanth KR (1987) Ground water assessment, development, and management. Tata McGraw-Hill Publishing Company Limited, New Delhi, p 720
- Kim Y, Lee K-S, Koh D-C, Lee D, Lee S, Park W, Koh G, Woo N (2003) Hydrogeochemical and isotopic evidence of groundwater salinization in a coastal aquifer: a case study in Jeju volcanic island, Korea. *J Hydrol* 270:282–294
- Koukadaki MA, Karatzas GP, Papadopoulou MP, Vafidis A (2007) Identification of the saline zone in a coastal aquifer using electrical tomography data and simulation. *Water Resour Manag* 21:1881–1898
- Lind CJ (1970) Specific conductance as a means of estimating ionic strength, in Geological Survey research 1970: U.S. Geological Survey Professional Paper 700-D, p. D272–D280
- Marimuthu S, Reynolds DA, Le Gal LC (2005) A field study of hydraulic, geochemical and stable isotope relationships in a coastal wetlands system. *J Hydrol* 315:93–116
- Mondal NC, Singh VS, Saxena VK, Prasad RK (2008) Improvement of ground water quality due to fresh water ingress in Potharlanka Island, Krishna delta, India. *Environ Geol* 55(3):595–603
- Mooney HM, Orellana E (1966) Master tables and curves for vertical electrical sounding over layered structures, Madrid Interciecia
- Mooney HM, Wetzel WW (1956) The potentials about a point electrode and apparent resistivity curves for a two, three and four layer earth. Univ. of Minnesota Press, Minneapolis, p 145
- Naik PK, Dehury BN, Tiwary AN (2007) Groundwater pollution around an industrial area in the coastal stretch of Maharashtra state, India. *Environ Monit Assess* 132:207–233. <https://doi.org/10.1007/s10661-006-9529-6>
- Nair IS, Parimala Renganayaki S, Elango L (2013) Identification of seawater intrusion by Cl/Br ratio and mitigation through managed aquifer recharge in aquifers North of Chennai, India. *J Groundw Res* 2:19
- Najib S, Fadili A, Mehdi K, Riss J, Makan A (2017) Contribution of hydrochemical and geoelectrical approaches to investigate salinization process and seawater intrusion in the coastal aquifers of Chaouia, Morocco. *J Contam Hydrol* 198(2017):24–36
- Narendra P, Rajendra Prasad P (2009) An empirical method for the 2D analysis of VES data. *J Appl Hydrol V–XVII(1 & 2)*:29–36
- Narendra P, Satyanarayana Tata (2007) Report on electrical resistivity surveys in the overexploited areas of Morshi and Warudtaluks, Amravati district (AAP 2006-07) CGWB technical report
- Orellana E, Mooney HM (1966) Master tables and curves for vertical electrical sounding over layered structures, Madrid Interciecia
- Piper AM (1944) A graphical procedure in the chemical interpretation of groundwater analysis. *Trans Am Geophys Union* 25:914–923
- Prasanna MV, Chidambaram S, ShahulHameed A, Srinivasamoorthy K (2010) Study of evaluation of groundwater in Gadilam basin using hydrogeochemical and isotope data. *Environ Monit Assess* 168:63–90
- Pujari P, Abhay K Soni (2009) Sea water intrusion studies near Kovaya limestone mine, Saurashtra coast, India. *Environ Monit Assess* 154:93–109. <https://doi.org/10.1007/s10661-008-0380-9>
- Rajkwaterstaat (1975) The standard graphs for resistivity prospecting. Publ. by the European Assoc. of Exploration Geophysists, Netherland

- Respond H (1990) Geoelektrische Untersuchungen zur Bestimmung der azwasserrSusswasser-Grenze im Gebiet zwischen Cuxhaven und Stade. *Geol Jahrb C* 56:3–37
- Richter BC, Krietler CW (1993) Geochemical techniques for identifying sources of ground-water salinisation. CRN Press Inc., Rotterdam, p 536
- Sabet MA (1975) Vertical electrical resistivity sounding locate ground-water resources: a feasibility study, Virginia Polytechnical Institute. *Water Resour Bull* 73:63
- Sathish S, Elango L, Rajesh R, Sarma VS (2011) Assessment of sea-water mixing in a coastal aquifer by high resolution electrical resistivity tomography. *Int J EnviSci Tech* 8(3):483–492
- Saxena VK, Krishna KVSS, Singh VS, Jain SC (2002) Hydro-chemical study for delineation of fresh groundwater region in the Potharlanka. Krishna Delta, India
- Saxena VK, Mondal NC, Singh VS (2004) Evaluation of hydrogeochemical parameters to delineate fresh groundwater zones in coastal aquifers. *J Appl Geochem* 6:245–254
- Saxena VK, Singh VS, Mondal NC, Maurya AK (2005) Quality of groundwater from Neil Island, Andaman & Nicobar, India. *J Appl Geochem* 7:201–206
- Senthilkumar S, Balasubramanian N, Gowtham B, Lawrence JF (2014) Geochemical signatures of groundwater in the coastal aquifers of Thiruvallur district, south India. *Appl Water Sci*. <https://doi.org/10.1007/s13201-014-0242-2>
- Senthilkumar S, Gowtham B, Sundararajan M, Chidambaram S, Francis Lawrence J, Prasanna MV (2017a) Impact of land use on the groundwater quality along coastal aquifer of Thiruvallur district, South India. *Sustain Water Resour Manag*. <https://doi.org/10.1007/s40899-017-0180-x>
- Senthilkumar S, Gowtham B, Vinodh K, Arulprakasam V, Sundararajan M (2017b) Delineation of geoelectric layers using imaging techniques in coastal blocks of Thiruvallur district, Tamil Nadu. *Indian J Geo Mar Sci* 46(05):986–994
- Singh KP (2003) A new approach for the detection of hidden aquifer using DC resistivity data transforms. *J GSI* 61:540–548
- Sivasubramanian P, Balasubramanian N, Soundranayagam JP, Chandrasekar N (2013) Hydrochemical characteristics of coastal aquifers of Kadaladi, Ramanathapuram district, Tamilnadu, India. *Appl Water Sci*. <https://doi.org/10.1007/s13201-013-0108-z>
- Store H, Storz W, Jacobs F (2000) Electrical resistivity tomography to investigate geological structures of earth's upper crust. *Geophys Prospect* 48:455–471
- Subba Rao N (2002) Geochemistry of groundwater in parts of Guntur district, A.P., India. *Environ Geol* 41:552–562
- Subramani T, Elango L, Damodarasamy SR (2005) Groundwater quality and its suitability for drinking and agricultural use in Chithar river basin, Tamil Nadu, India. *J Environ Geol* 47:1099–1110
- Telford WM, Geldart LP, Sheriff RE (1990) Applied geophysics. Cambridge University Press, Cambridge
- Thilagavathi R, Chidambaram S, Prasanna MV, Thivya C, Singaraja C (2012) A study on groundwater geochemistry and water quality in layered aquifers system of Pondicherry region, southeast India. *Appl Water Sci* 2:253–269. <https://doi.org/10.1007/s13201-012-0045-2>
- UNDP (1987) Hydro geological and artificial recharge studies, Madras. Technical report, UNDP, Report number DP/UN/IND-78-029/2
- Vandenbohede A, Courtens C, William de Breuck L (2010) Fresh-salt water distribution in the central Belgian coastal plain: an update. *Geol Belg* 11(3):163–172
- Worthington PF (1977) Influence of matrix conduction upon hydrogeological relationship in arenaceous aquifers. *Water Res* 13(1):87–92
- Yadav GS, Abolfazli H (1998) Geoelectrical soundings and their relationship to hydraulic parameters in semiarid regions of Jalore, northwestern India. *J Appl Geophys* 39:35–51
- Zohdy AAR (1969) The use of Schlumberger and equatorial soundings in groundwater investigations near El Paso, Texas. *Geophysics* 34:713–728
- Zohdy AAR (1974) Application of surface geophysics to groundwater investigations, USGS, Washington DC

Publisher's Note Springer Nature remains neutral with regard to jurisdictional claims in published maps and institutional affiliations.